

Supporting Information

Photoluminescent and magnetic analysis of a family of lanthanide(III) complexes based on diclofenac

E. Echenique-Errandonea,^a I. Oyarzabal,^a J. Cepeda,^a E. San Sebastian,^a A. Rodríguez-Díéguez^{*b} and J. M. Seco^{*a}

^a Departamento de Química Aplicada, Facultad de Química, Universidad del País Vasco/Euskal Herriko Unibertsitatea, UPV/EHU, 20018, San Sebastián, Spain. ^b

Departamento de Química Inorgánica, Universidad de Granada, 18071, Granada, Spain.

Index:

- 1. Elemental Analyses and Bond lengths and angles.**
- 2. Additional Figures.**
- 3. Experimental PXRD.**
- 4. Continuous Shape Measurements.**
- 5. Magnetic Properties**
- 6. Luminescence Properties.**
- 7. TD-DFT calculations.**

1. Elemental Analyses and Crystallographic Tables.

Table S.1. Yields and elemental analyses for complexes **1-10**.

Complex	Yield (%)	Formula	%C calc./found	%H calc./found	%N calc./found
1	68.47	C ₈₆ H ₇₂ Cl ₁₂ Pr ₂ N ₆ O ₁₆	46.62/46.73	2.99/3.05	3.92/3.85
2	60.47	C ₈₆ H ₇₂ Cl ₁₂ Nd ₂ N ₆ O ₁₆	46.61/46.75	2.98/3.03	3.94/3.88
3	67.90	C ₈₆ H ₇₂ Cl ₁₂ Sm ₂ N ₆ O ₁₆	47.38/47.56	2.95/3.34	3.95/3.87
4	68.33	C ₈₆ H ₇₂ Cl ₁₂ Eu ₂ N ₆ O ₁₆	47.37/47.49	3.06/3.34	3.88/3.86
5	67.89	C ₈₆ H ₇₂ Cl ₁₂ Tb ₂ N ₆ O ₁₆	47.15/47.19	3.17/3.32	3.89/3.84
6	65.30	C ₈₆ H ₇₂ Cl ₁₂ Dy ₂ N ₆ O ₁₆	46.98/47.04	3.14/3.30	3.90/3.83
7	67.58	C ₈₆ H ₇₂ Cl ₁₂ Ho ₂ N ₆ O ₁₆	46.87/46.93	2.98/3.30	3.87/3.82
8	63.56	C ₈₆ H ₇₂ Cl ₁₂ Er ₂ N ₆ O ₁₆	46.75/46.83	3.10/3.29	3.86/3.81
9	61.86	C ₈₆ H ₇₂ Cl ₁₂ Tm ₂ N ₆ O ₁₆	46.58/46.76	3.24/3.29	3.83/3.80
10	68.89	C ₈₆ H ₇₂ Cl ₁₂ Yb ₂ N ₆ O ₁₆	46.42/46.59	3.08/3.27	3.85/3.79

Table S2.- Bond lengths (\AA) and angles ($^\circ$) for compounds **1** and **6**.

Bond distances (\AA)	1	6
Ln1---O1A	2.501	2.414
Ln1---O2A	2.504	2.430
Ln1---O1B	2.521	2.450
Ln1---O2B	2.593	2.491
Ln1---O1C	2.528	2.442
Ln1---O2C	2.421	2.329
Ln1---O2C'	2.619	2.548
Ln1---O1M	2.487	2.375
Ln1---O1W	2.475	2.361
Ln1---Ln1'	4.513	4.059
Bond angles ($^\circ$)		
O1A--- Ln1---O2A	52.11	53.67
O1B--- Ln1---O2B	51.15	52.84
O1C--- Ln1---O2C	50.46	51.87
O2C--- Ln1---O2C'	69.09	67.39
Ln1---O2C---Ln1'	110.91	112.61
O1W---Ln1---O1M	83.88	82.63

Table S3.Structural parameters of hydrogen bonds (\AA , $^\circ$) in compound **1**.^a

$D-H\cdots A^b$	$D-H$	$H\cdots A$	$D\cdots A$	$D-H\cdots A$
O1w-H1wa…O1B(i)	0.88	1.91	2.741(2)	155.8
O1w-H1wb…O1A(i)	0.88	1.94	2.758(2)	153.1

^aSymmetry codes: (i) $-x, -y, -z$. ^bD: donor. A: acceptor.

Table S4.Structural parameters of hydrogen bonds (\AA , $^\circ$) in compound **6**.^a

$D-H\cdots A^b$	$D-H$	$H\cdots A$	$D\cdots A$	$D-H\cdots A$
O1w-H1wa…O1A(i)	0.85	2.02	2.830(5)	159.7
O1w-H1wb…O1B(i)	0.85	1.99	2.743(4)	145.7

^aSymmetry codes: (i) $-x, -y, -z$. ^bD: donor. A: acceptor.

2. Additional Figures.

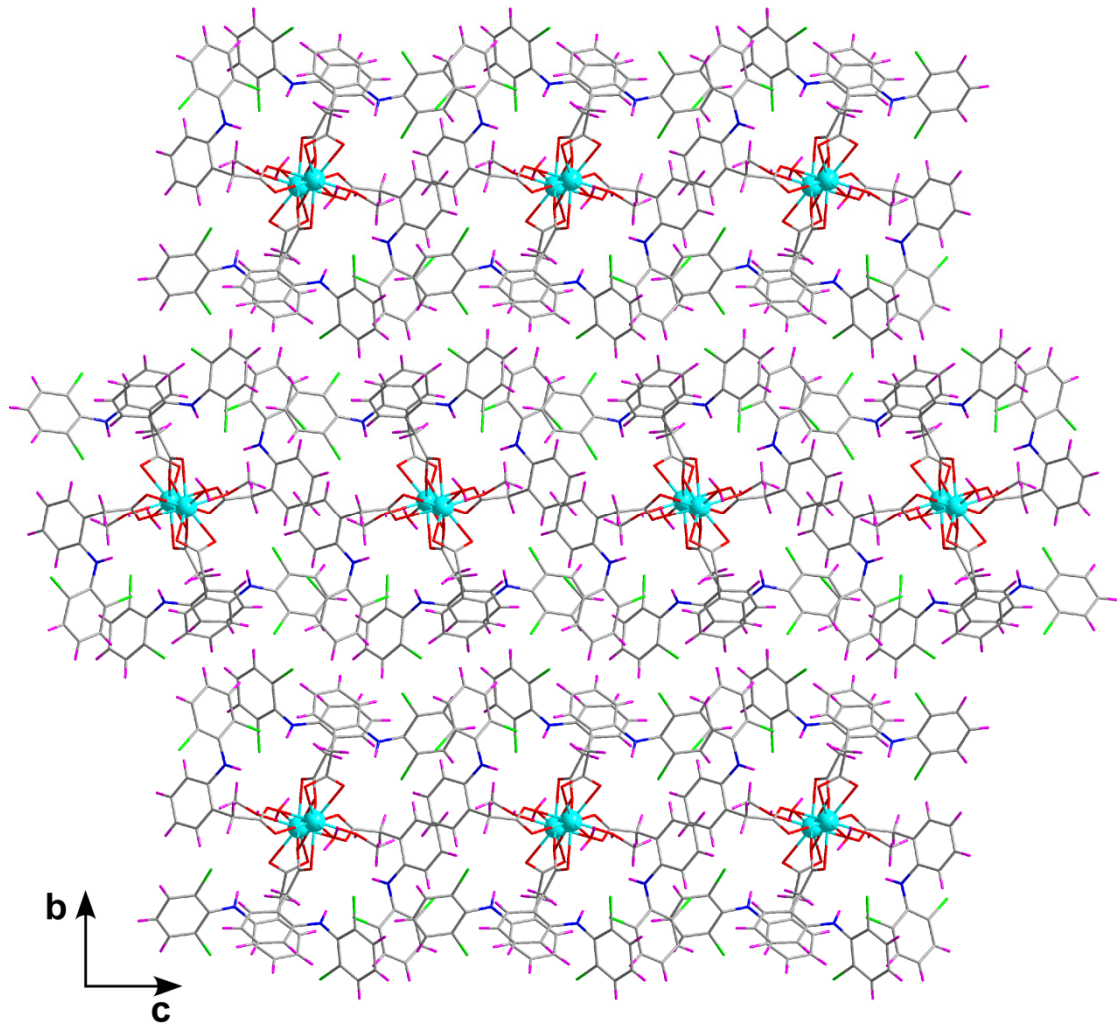
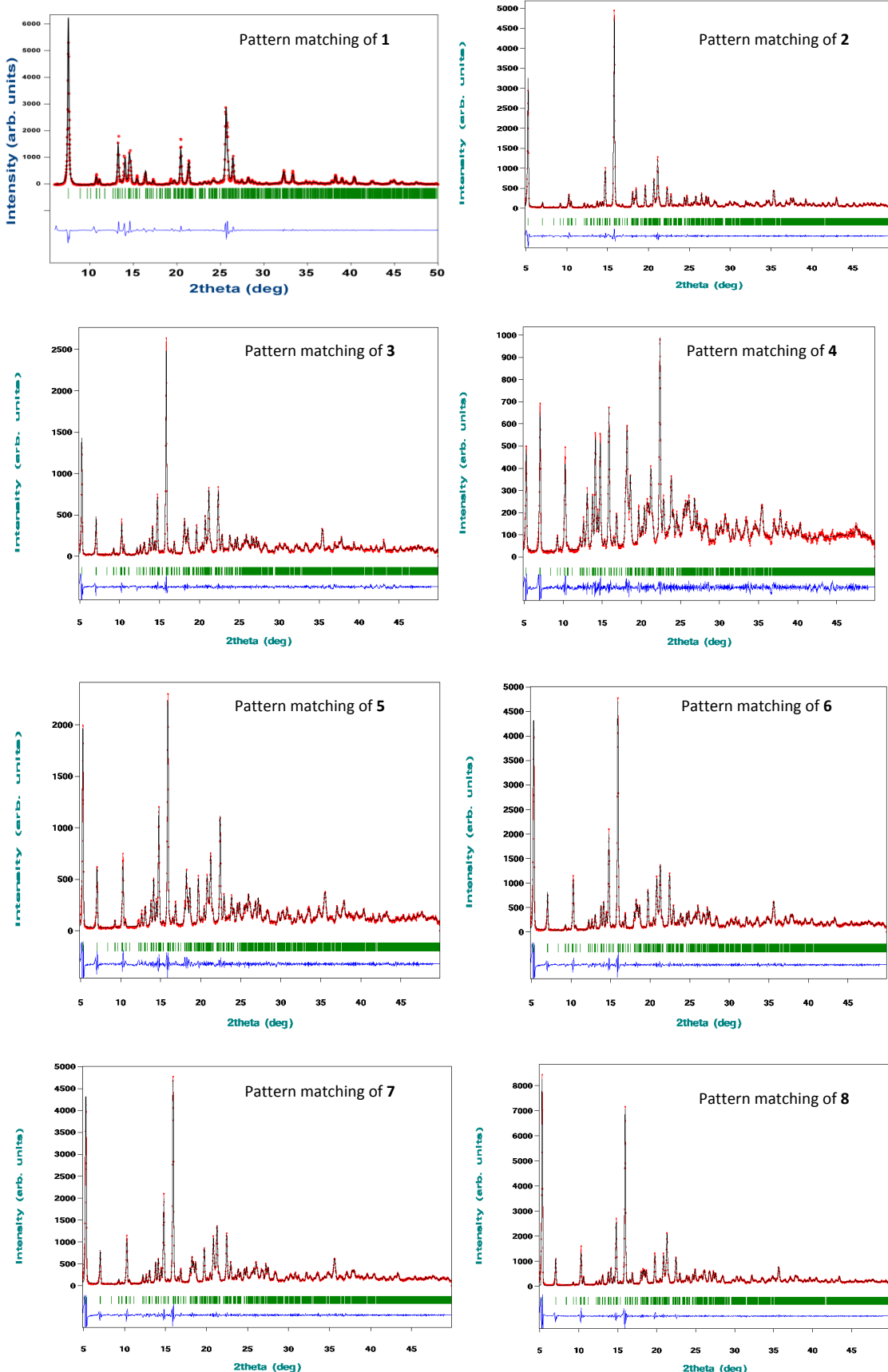


Figure S1.- View of the 3D packing of chains in complex **1** along the crystallographic *bc* plane.

3. Experimental XRPD.



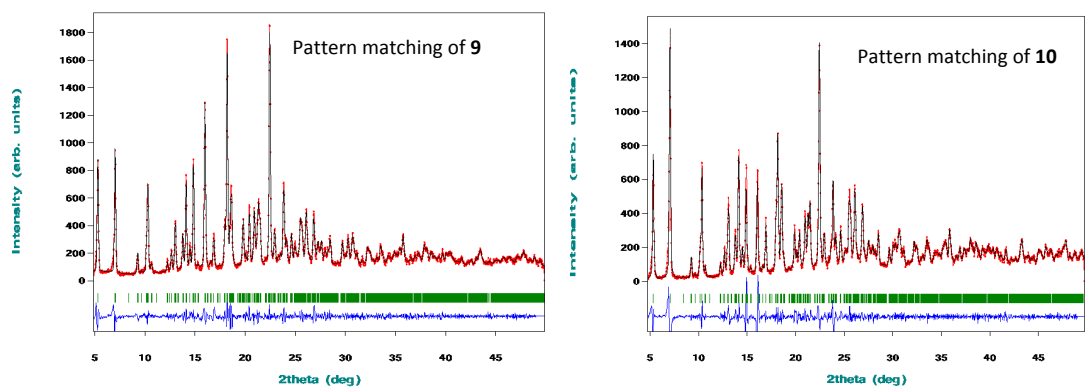


Figure S2.- Pattern-matching analyses and experimental PXRD for complexes **1-10**.

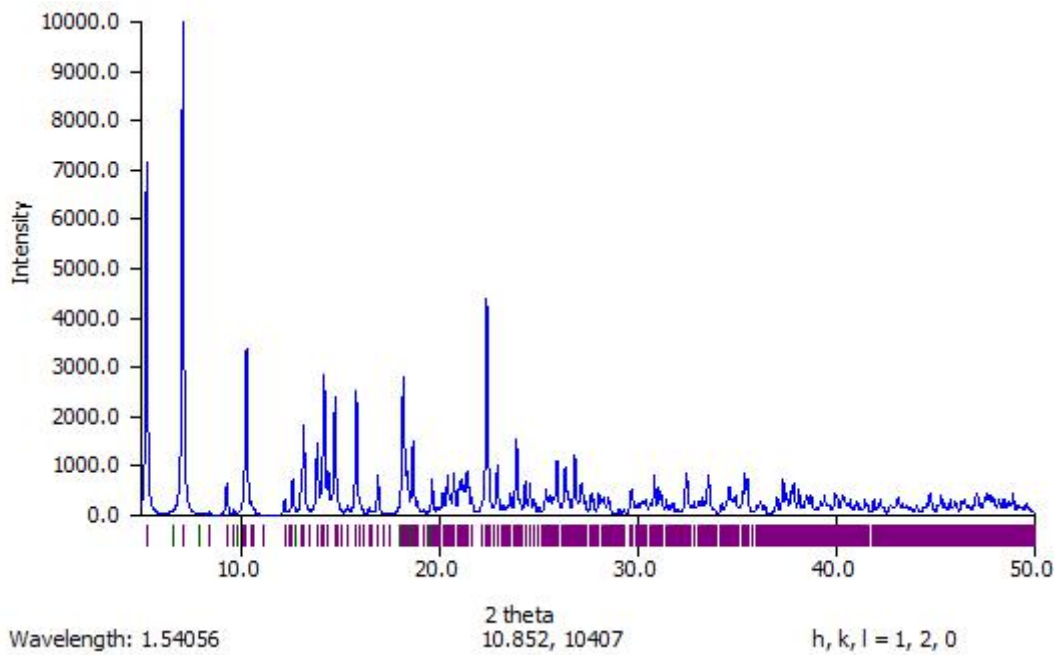


Figure S3.- Theoretical XRPD spectra of complex **1**. Complexes **1-10** were compared with this theoretical spectrum.

4. Continuous Shape Measurements.

Table S5.- Continuous Shape Measurements for the LnO₉ coordination environment.

EP-9	1 D9h	Enneagon
OPY-9	2 C8v	Octagonal pyramid
HBPY-9	3 D7h	Heptagonal bipyramid
JTC-9	4 C3v	Johnson triangular cupola J3
JCCU-9	5 C4v	Capped cube J8
CCU-9	6 C4v	Spherical-relaxed capped cube
JCSAPR-9	7 C4v	Capped square antiprism J10
CSAPR-9	8 C4v	Spherical capped square antiprism
JTCTPR-9	9 D3h	Tricapped trigonal prism J51
TCTPR-9	10 D3h	Spherical tricapped trigonal prism
JTDIC-9	11 C3v	Tridiminished icosahedron J63
HH-9	12 C2v	Hula-hoop
MFF-9	13 Cs	Muffin

Complex	JCSAPR-9	CSAPR-9	TCTPR-9	MFF-9
1	3.786	2.639	2.842	2.519
6	3.594	2.497	2.653	2.228

5. Magnetic Properties.

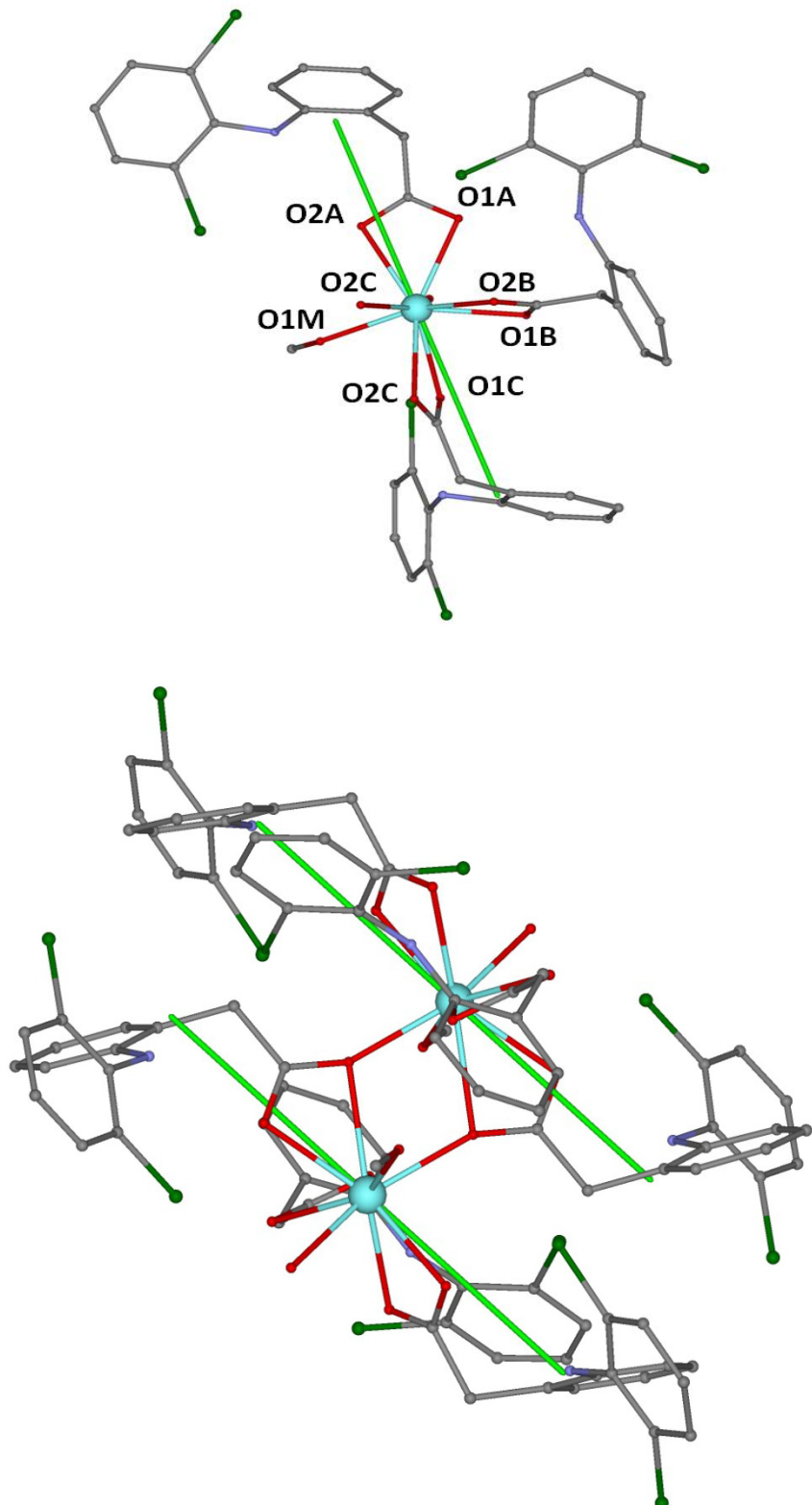


Figure S4.- Theoretical orientation of the magnetic moments (green line) for Dy^{III} ions in complex **6**. The upper figure shows the asymmetrical unit.

6. Luminescence Properties.

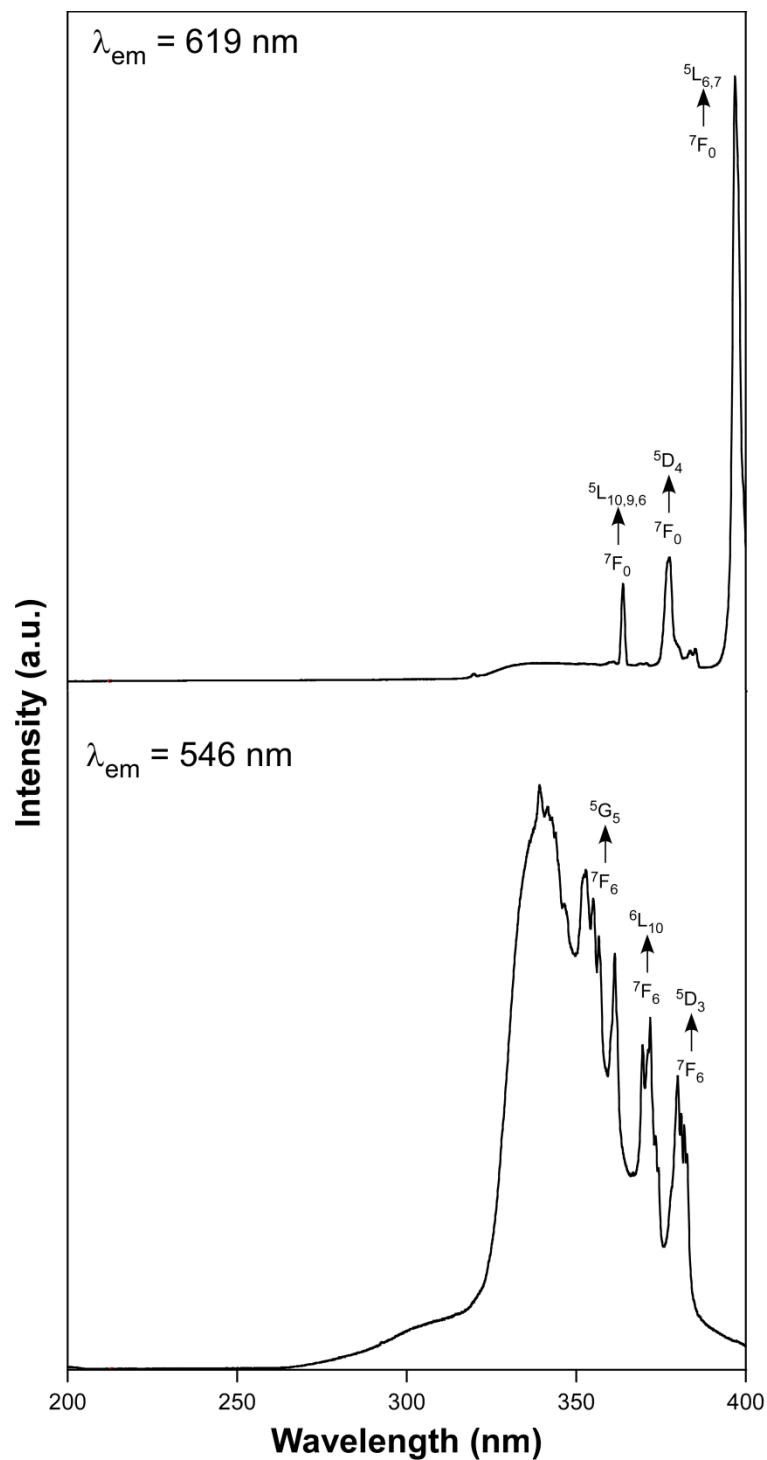


Figure S5.- Excitation spectra monitored at 619 nm for **4** (top) and 546 nm for **5** (down) compounds recorded at 10 K.

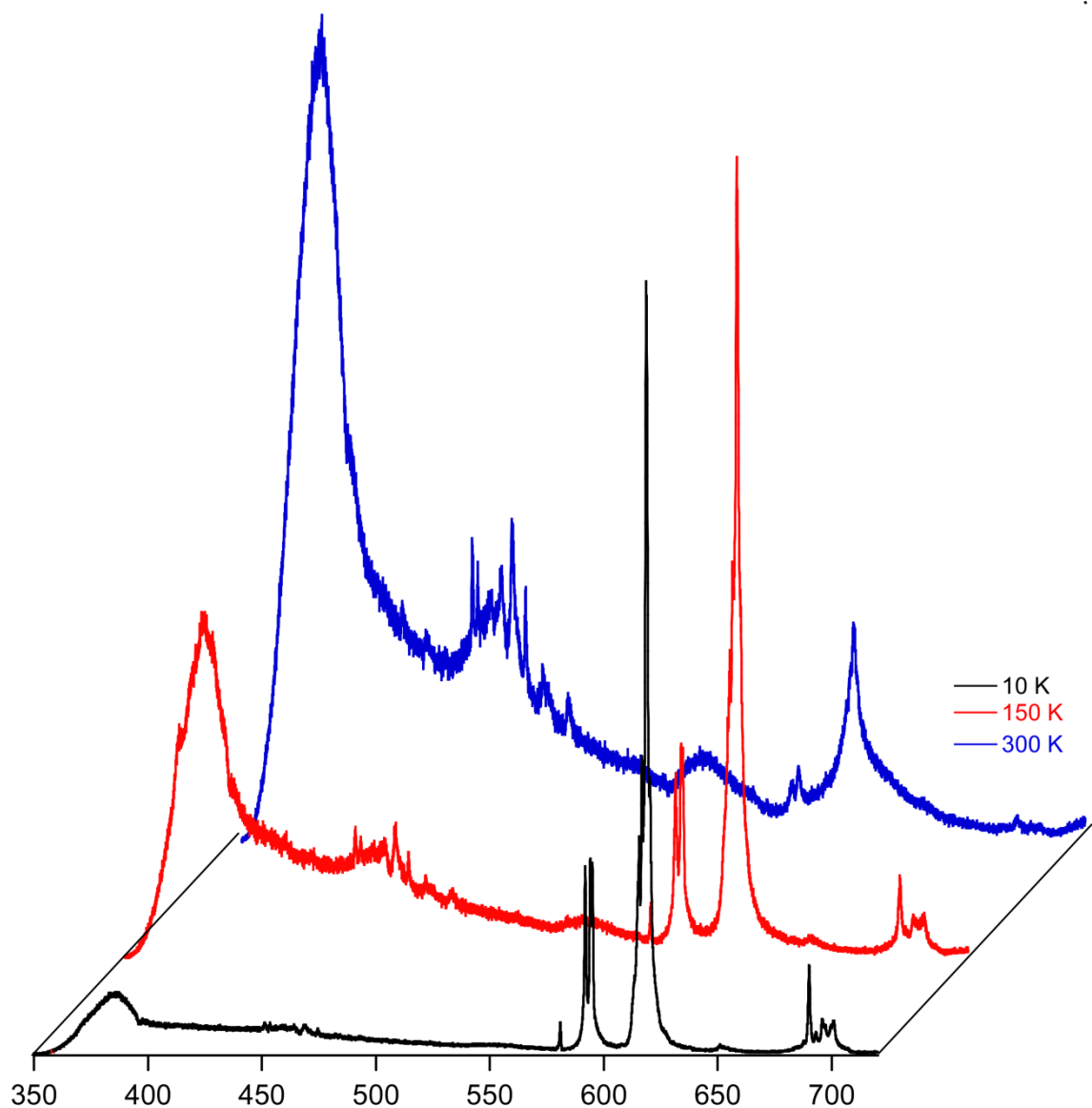


Figure S6.- Thermal evolution of the emission spectrum of compound **4** excited at 325 nm.

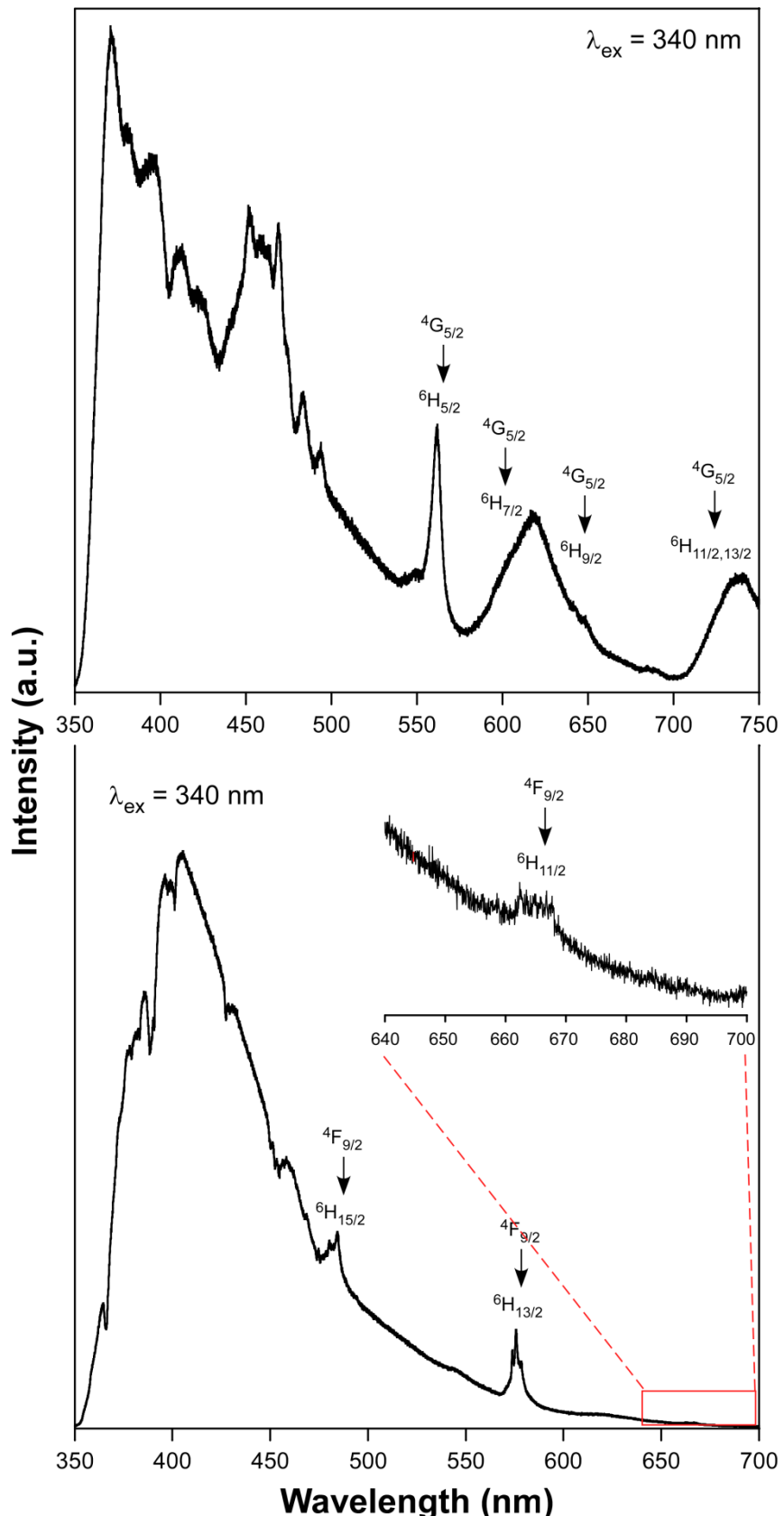


Figure S7.- Emission spectra at 10 K for **3** (top) and **6** (down). The inset shows magnified image of the weakest emission band corresponding to the: $^4\text{F}_{9/2} \rightarrow ^6\text{H}_{11/2}$ transition.

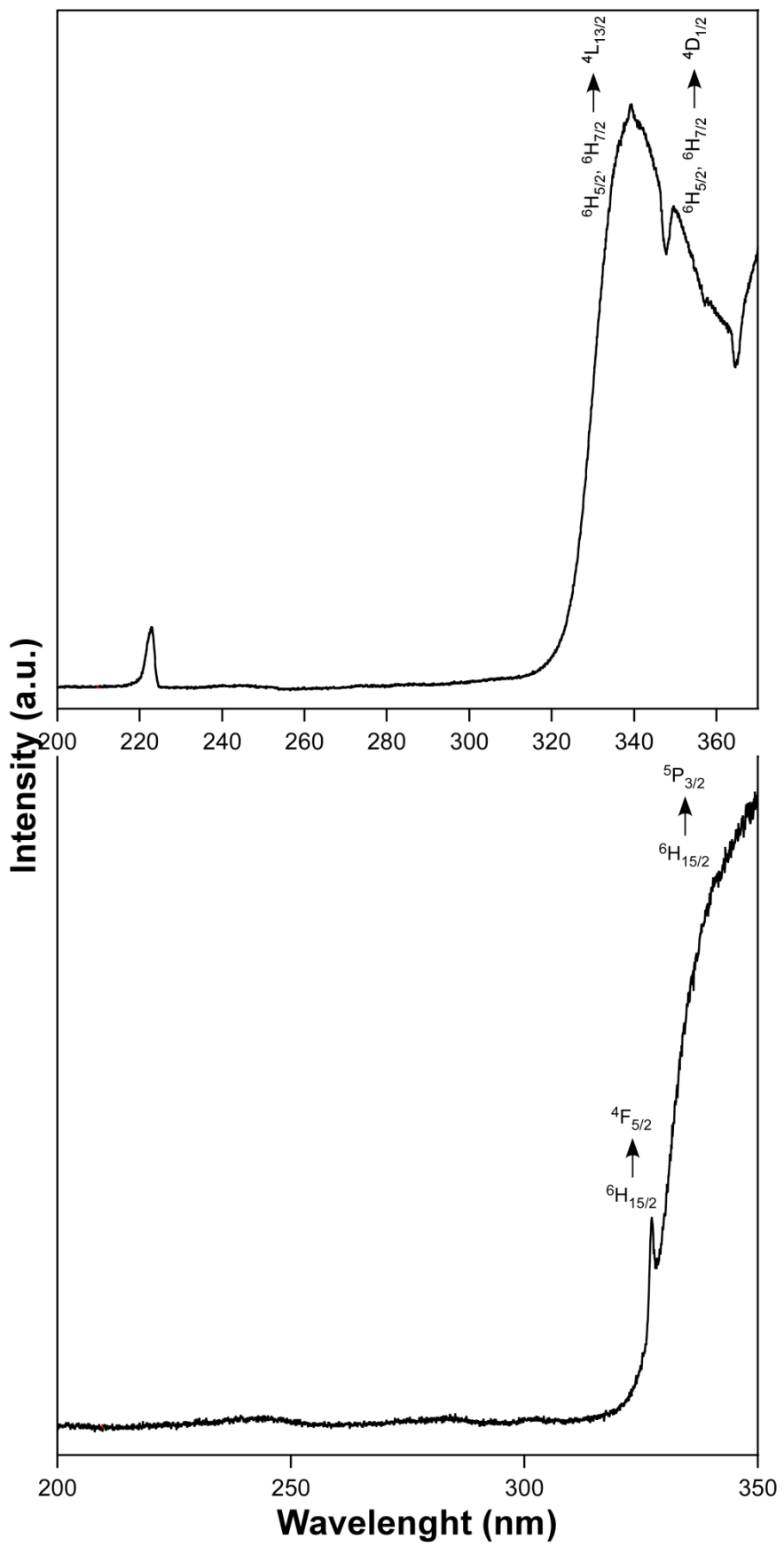


Figure S8.- Excitation spectra at 10 K for **3** (top) and **6** (down) focusing at 562 and 480 nm, respectively.

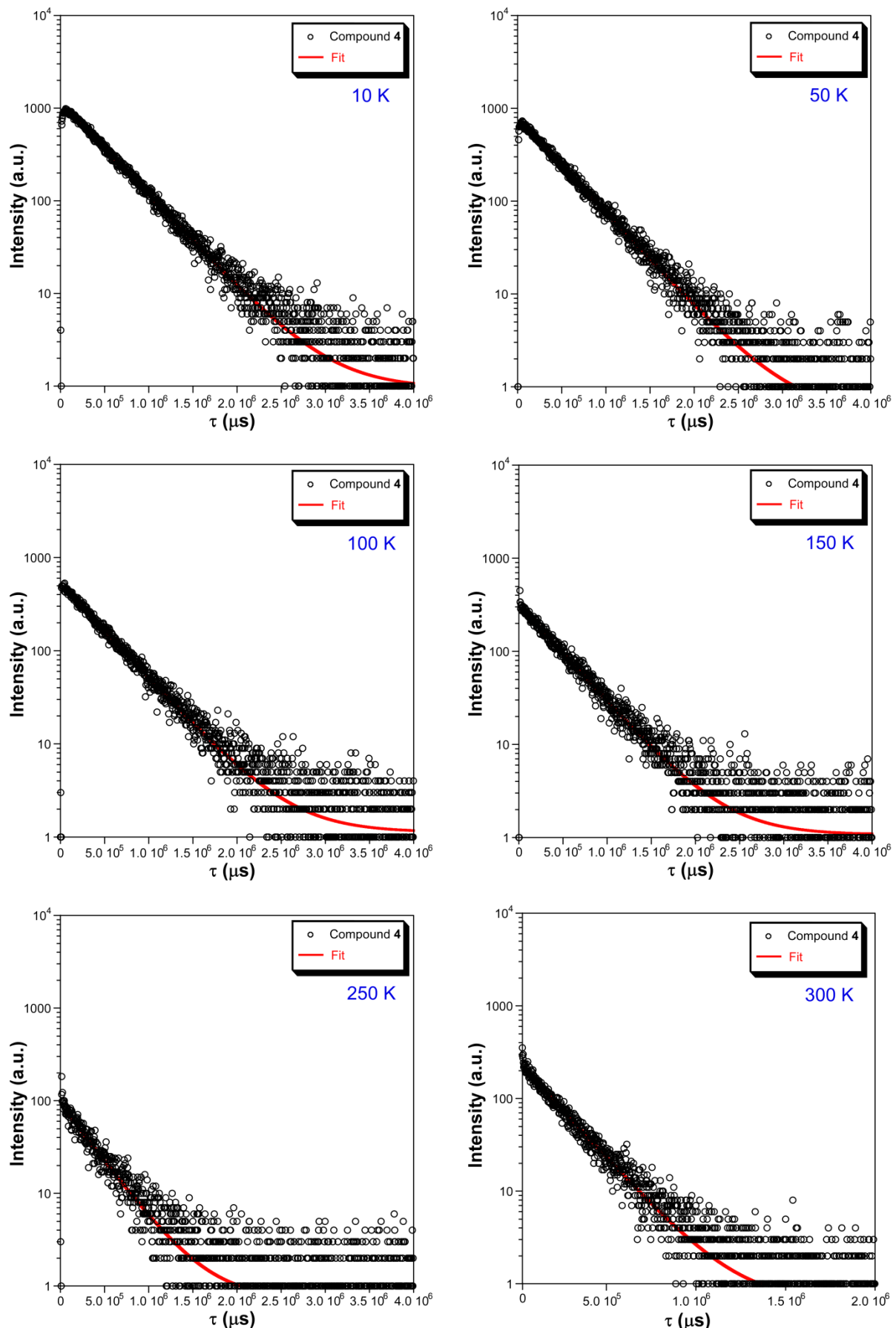


Figure S9.- Luminescence decay lifetime fits of **4** (Eu) monitored at ${}^5\text{D}_0 \rightarrow {}^7\text{F}_2$ transition.

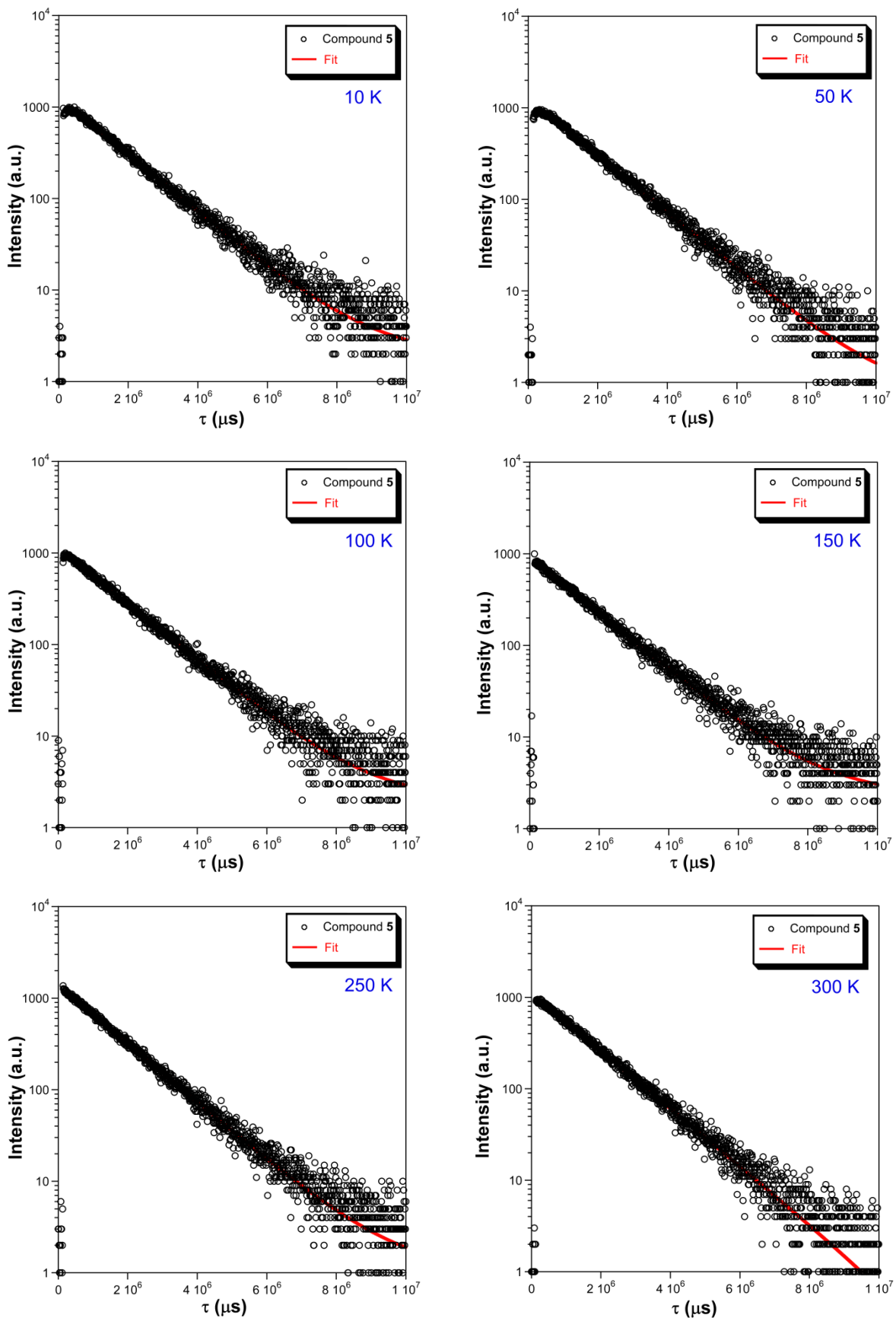


Figure S10.- Luminescence decay lifetime fits of **5** (Tb) monitored at ${}^5D_4 \rightarrow {}^7F_5$ transition.

7. TD-DFT calculations.

Table S6. Calculated main excitation energies (nm) and singlet electronic transitions and associated oscillator strengths of diclofenac molecule in gas phase.

Calcd. λ (nm)	Exp. λ (nm)	Significant contributions	Osc. strength (a.u.)
213	220	HOMO – 6 \rightarrow LUMO (32%) HOMO – 3 \rightarrow LUMO + 4 (51%) HOMO – 4 \rightarrow LUMO + 3 (8%)	0.1681
221	220	HOMO – 6 \rightarrow LUMO (23%) HOMO – 5 \rightarrow LUMO + 1 (47%) HOMO – 3 \rightarrow LUMO + 4 (22%)	0.0538
310	330	HOMO – 3 \rightarrow LUMO + 1 (91%) HOMO – 2 \rightarrow LUMO + 4 (4%)	0.1303
321	330	HOMO – 2 \rightarrow LUMO + 3 (82%) HOMO – 3 \rightarrow LUMO + 1 (4%) HOMO – 2 \rightarrow LUMO + 4 (3%)	0.0407

Table S7. Calculated main emission energies (nm) and singlet electronic transitions and associated oscillator strengths of diclofenac molecule in gas phase.

Calcd. λ (nm)	Exp. λ (nm)	Significant contributions	Osc. strength (a.u.)
370	386	HOMO – 3 \leftarrow LUMO + 1 (96%)	0.0844
365	386	HOMO – 3 \leftarrow LUMO + 1 (96%)	0.0681
486	462	HOMO – 2 \leftarrow LUMO + 1 (94%) HOMO \leftarrow LUMO + 2 (5%)	0.0099

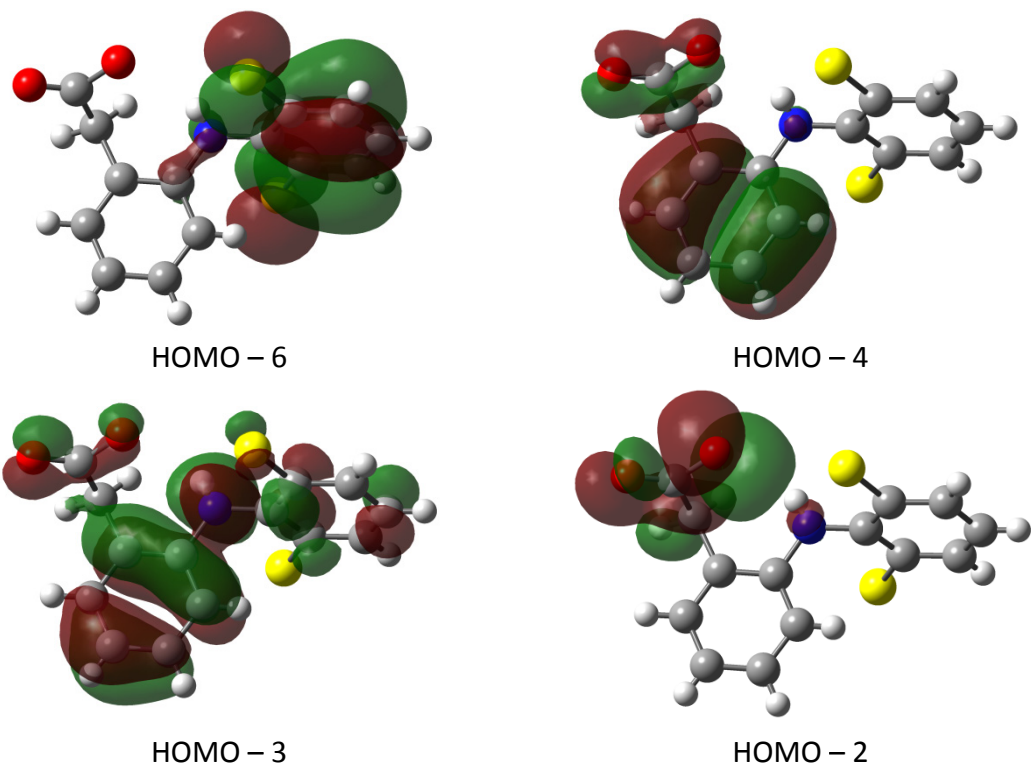


Figure S11.- Highly Occupied Molecular Orbitals of diclofenac molecule involved in the singlet excitation transitions.

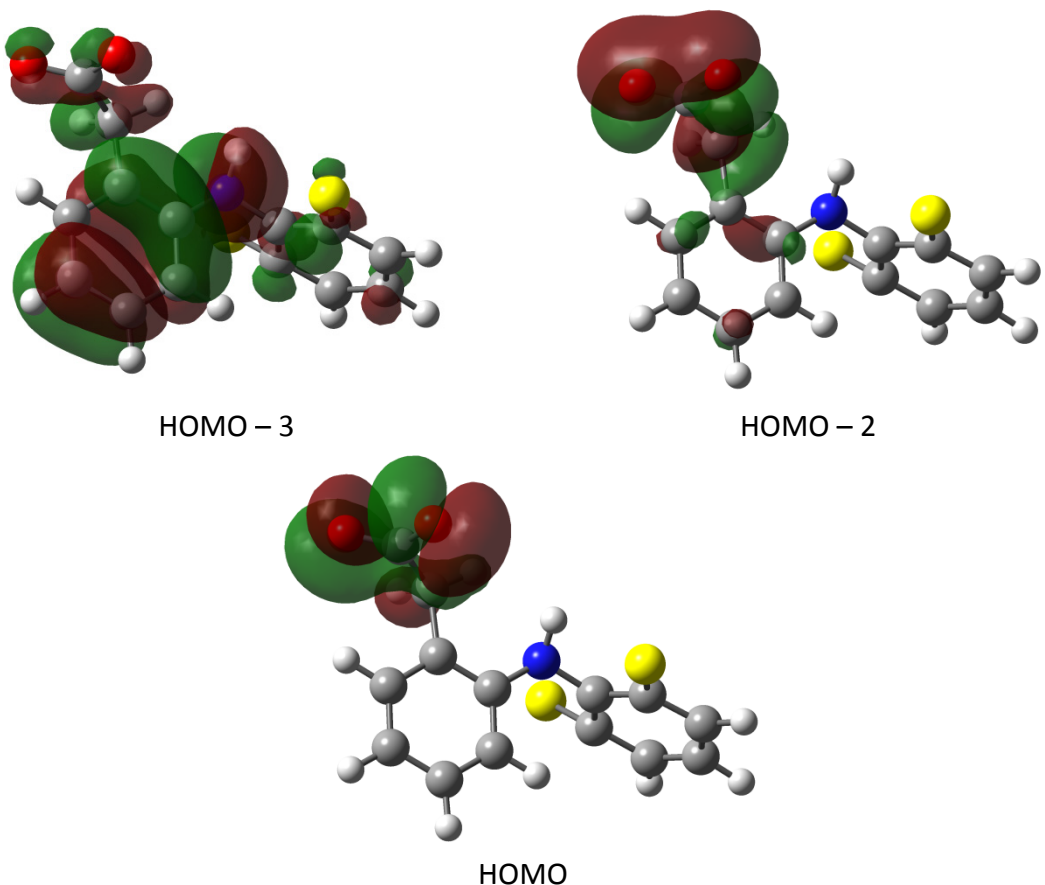


Figure S12.- Highly Occupied Molecular Orbitals of diclofenac molecule involved in the singlet emission transitions.

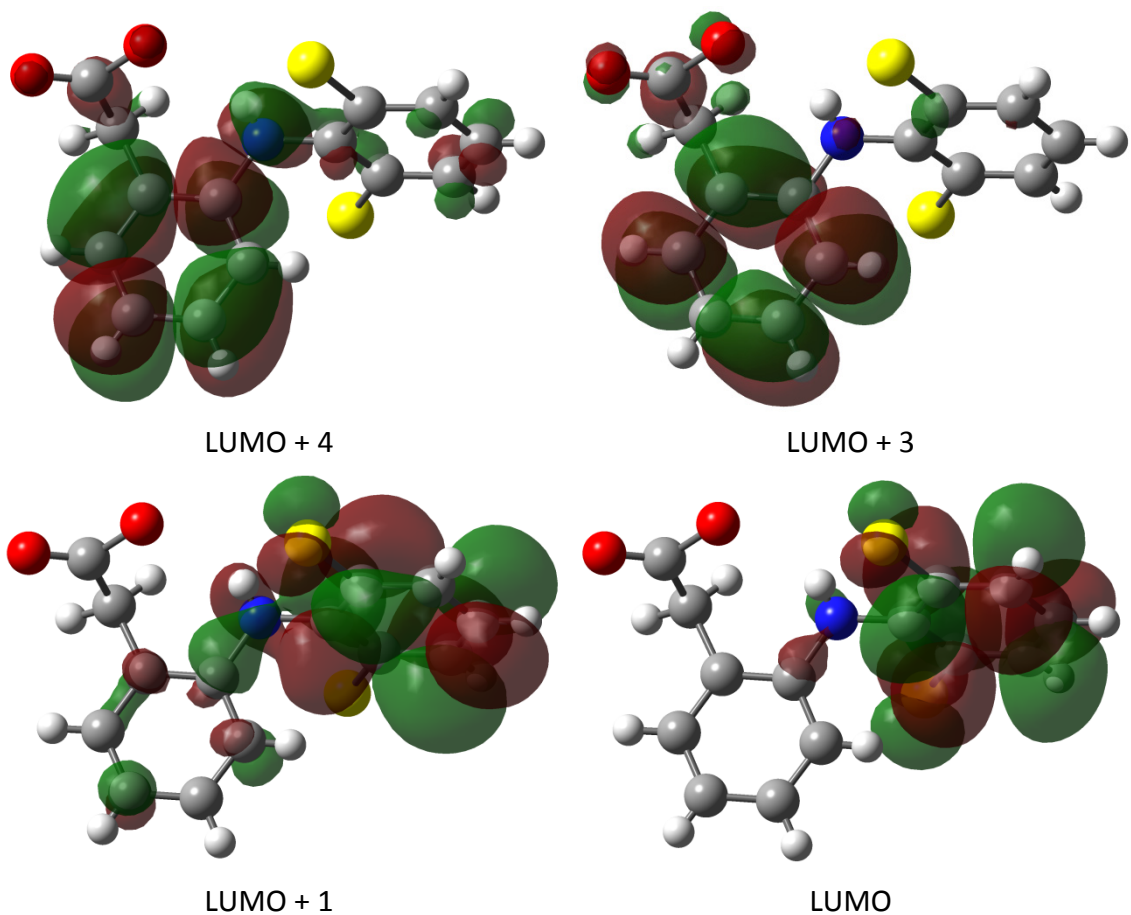


Figure S13.- Lowest Unoccupied Molecular Orbitals of diclofenac molecule involved in the singlet excitation transitions.

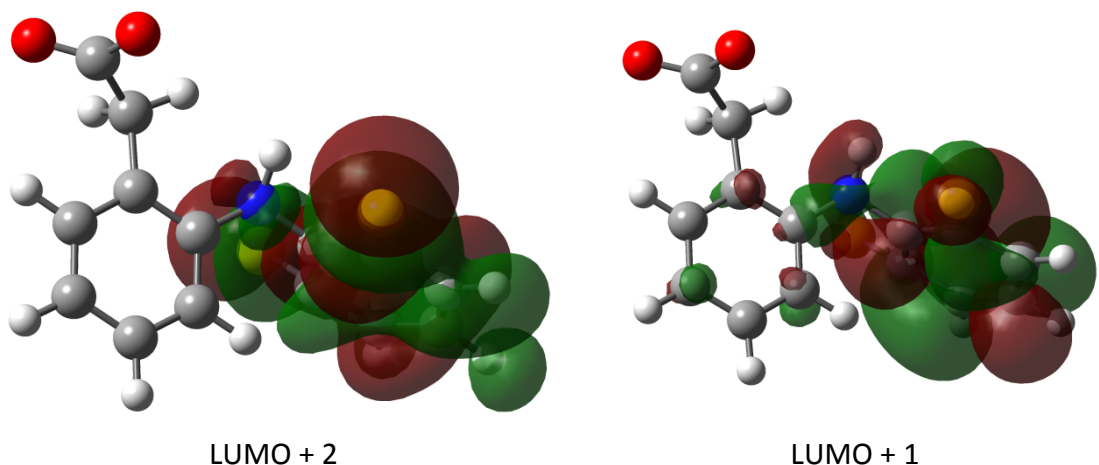


Figure S14.- Lowest Unoccupied Molecular Orbitals of diclofenac molecule involved in the singlet emission transitions.